

Comparison of the isolated-resonance approximation and multichannel quantum-defect theory for dielectronic recombination

K. LaGattuta and Y. Hahn

Department of Physics, University of Connecticut, Storrs, Connecticut 06268

(Received 20 March 1984)

The effect of overlapping resonances on dielectronic recombination cross sections and rate coefficients is examined using a simple two-channel model. Results obtained by multichannel quantum-defect theory and the isolated-resonance approximation are found to be closely similar, for realistic choices of scattering parameters and of radiative widths; i.e., except just below threshold where resonances strongly overlap.

I. INTRODUCTION

The importance of the dielectronic-recombination (DR) process in low-density, high-temperature plasmas has been recognized since the work of Burgess¹ in the early 1960's. Over the past 20 years, many calculations of DR rate coefficients (α^{DR}) for ions of coronal significance, and more recently for ions occurring in fusion plasmas, have been performed. Usually, such work makes use of the isolated-resonance approximation (IRA), combined with either distorted-wave^{2,3} (DW) or close-coupling theories. However, approaches based upon configuration interaction (CI) with the continuum,⁴ or the multichannel quantum-defect theory (MQDT) of Seaton⁵ are possible; see the review article by Seaton and Storey.⁶

In practice, the MQDT and CI methods have been applied to the study of the structure of only limited numbers of interacting DR resonances. It has proved difficult to apply these procedures systematically over an entire DR energy range, where hundreds or perhaps thousands of resonances can appear. In particular, MQDT is not easily applied when states of very low n are involved or where radiative widths are large. Hence rate coefficients, which involve a sum over the entire spectrum of resonances, have not been produced in quantity by these methods. Instead, the more manageable IRA has been used extensively to provide these α^{DR} values.^{7,8}

The IRA may seem suspect, however, when either the Auger width (Γ_a) or the radiative width (Γ_r) becomes comparable to, or greater than, the spacing between adjacent resonances. This can be the case and could lead to important corrections to α^{DR} if, for instance, (1) the ionic charge (Z_I) is large, and a continuum electron of large orbital angular momentum is captured to a moderately high Rydberg state (HRS), or (2) Z_I is small, and a continuum electron is captured to a very HRS.

Recently, a model calculation of the DR cross section (σ^{DR}), based upon MQDT, has appeared.⁹ This model is simple, and σ^{DR} can be obtained from it analytically, for all values of the energy, and for all values of Γ_r . Most importantly, σ^{DR} can be computed in both the isolated resonance regime, and in the region of energies where the resonances are overlapping.

In the following, we compare the detailed predictions of this model, based upon MQDT, with an IRA calculation for the same model system. As will be seen, the two theories yield closely similar results except when resonances overlap.

We describe the model in Sec. II. In Sec. III A we apply MQDT to the model system, and examine the properties of the derived σ^{DR} . Section III B considers the characteristics of the IRA, when applied to the same model system. Sections IV A and IV B describe σ^{DR} values obtained over ranges of the model parameters for the MQDT and the IRA, respectively. A comparison of the two approaches appears in Sec. V.

II. THE MODEL

The object here is to reduce to its essential features the DR process, described by

$$e^-(k_c, l_c) + A^{+Z_I} \rightleftharpoons A^{+(Z_I-1)**} \rightarrow A^{+(Z_I-1)*} + \gamma, \quad (1)$$

where A^{+Z_I} is any Z_I -times ionized atom, $e^-(k_c, l_c)$ represents a continuum electron of energy k_c^2 (Ry) and orbital angular momentum l_c , γ denotes an emitted photon, and * indicates an excited state of the recombined ion (single or double excitation). Following Ref. 9, we consider a two-state target, for which both the ground and excited states are s states; we assume further that only the continuum $l_c=0$ partial wave can produce a target excitation. Therefore, the continuum electron is always captured into an s state. The reaction (1) becomes

$$e^-(k_c, l_c=0) + n'_i s \rightleftharpoons (n'_d s)(ns) \rightarrow (n'_i s)(ns) + \gamma, \quad (2)$$

where n'_i and n'_d are the initial- and intermediate-state principal quantum numbers, respectively, for the active electron of the target, and where "radiative" stabilization occurs via an s to s transition. The difference between the target energies is labeled Δ (Ry). Throughout, spin is ignored.

Just above the threshold for target excitation, $k_c^2 \gtrsim \Delta$, the R -matrix elements describing the scattering are approximated by real constants, $R_{11} \equiv \beta$, $R_{22} \equiv \alpha$, and $R_{12} = R_{21} \equiv \gamma$, where α , β , and γ are arbitrary parameters

within the model. Further, it is assumed that for all $k_c^2 < \Delta$ these constants remain invariant. Finally, the radiative probability Γ_r is defined as another arbitrarily chosen constant in the model. The model contains altogether four free parameters.

III. THE TWO THEORIES

A. MQDT

Below the threshold for inelastic scattering, the elastic phase shift η is given (in MQDT) by⁵

$$\eta = \tan^{-1} \{ \beta - \gamma [\tan(\pi Z) + \alpha]^{-1} \gamma \}, \quad (3)$$

where

$$Z = 1 / [(\Delta - k_c^2)]^{1/2}. \quad (4)$$

The elastic S -matrix element is, as usual,

$$S = e^{2i\eta}, \quad (5)$$

while the cross section for elastic scattering is

$$\sigma_{el} = \frac{\pi}{k_c^2} |1 - S|^2. \quad (6)$$

It is a consequence of (3) that σ_{el} shows characteristic peaks due to resonance scattering (unless $\alpha \approx \beta$, when $|\alpha| \gg 1$).

The inelastic cross section, given by

$$\sigma_{inel} = \frac{\pi}{k_c^2} (1 - |S|^2), \quad (7)$$

is zero for $k_c^2 < \Delta$, unless $\Gamma_r \neq 0$. For nonzero Γ_r , we add a negative imaginary part to the excited-state energy;⁹ viz.,

$$\Delta \rightarrow \Delta - i\Gamma_r/2. \quad (8)$$

Upon making this substitution, $|S| < 1$, and then $\sigma_{inel} \neq 0$. Here, Γ_r (Ry) models the radiative decay of the inner-shell electron; the HRS electron decay is too slow to be important. However, both of these possibilities are included in a more general way in Ref. 10.

To simplify matters further, we require additionally that $\det R = 0$, or $\alpha\beta = \gamma^2$. Now, Eqs. (3), (5), and (8) taken together yield

$$\sigma_{inel} = 4\alpha\beta B / [(\beta B + \alpha + A)^2 + (B - \beta A)^2], \quad (9)$$

where

$$\tan(\pi Z) \equiv A + iB \quad (10)$$

and both A and B are real functions of k_c^2 . The S -matrix element itself is given by

$$S = \frac{(1+i\beta)\tan(\pi Z) + \alpha}{(1-i\beta)\tan(\pi Z) + \alpha}. \quad (11)$$

$$\sigma_{inel} = \frac{2\pi}{k_c^2} \alpha\beta \sinh(2x_-) (\cos^2 x_+ + \sinh^2 x_-) \{ \alpha^2 (\cos^2 x_+ + \sinh^2 x_-)^2 + \alpha [\sin(2x_+) + \beta \sinh(2x_-)] (\cos^2 x_+ + \sinh^2 x_-) + \frac{1}{4} (1 + \beta^2) [\sin^2(2x_+) + \sinh^2(2x_-)] \}^{-1}, \quad (18)$$

This function has simple poles at values of $Z = Z_n$, where n is an integer greater than or equal to 1, and

$$Z_n = n + \frac{1}{2\pi} \tan^{-1} \left[\frac{-2\alpha}{1 + \beta^2 - \alpha^2} \right] - \Theta(\text{Re} Z_n) + \frac{i}{2\pi} \ln \left| \frac{[1 + 2(\alpha^2 + \beta^2) + (\alpha^2 - \beta^2)^2]^{1/2}}{1 + (\alpha + \beta)^2} \right|, \quad (12)$$

where $\Theta(x) = 1$ for $x \geq 0$, and $\Theta(x) = 0$ for $x < 0$. For $Z \approx Z_n$, one has that

$$S \approx \frac{-4i\alpha\beta / [\alpha^2 + (1 - i\beta)^2]}{\left[k_c^2 - \Delta + \frac{1}{Z_n^2} + \frac{i\Gamma_r}{2} \right] \pi Z_n^3}. \quad (13)$$

The Z_n values determine both the quantum defects μ_n , and the Auger widths $\Gamma_a(n)$ (Ry). The effective quantum number n^* is related to the quantum defect by

$$n^* = n - \mu_n \quad (14)$$

while

$$n^* = \text{Re} Z_n. \quad (15)$$

The Auger width is given by

$$\Gamma_a(n) \approx -4 \frac{\text{Im} Z_n}{(n^*)^3} \quad (16)$$

provided that $\text{Im} Z_n \ll n^*$.

B. IRA

According to a well understood prescription,^{2,6} the DR cross section, in the isolated-resonance approximation, is given by

$$\sigma^{\text{DR}} = \frac{\pi}{k_c^2} \Gamma_r \sum_{n=n_0}^{\infty} \frac{\Gamma_a(n)}{\left[\left[k_c^2 - \Delta + \frac{1}{n^{*2}} \right]^2 + \frac{1}{4} [\Gamma_r + \Gamma_a(n)]^2 \right]}. \quad (17)$$

In evaluating this expression we take model values of Γ_r , and values of n^* and $\Gamma_a(n)$ given by Eqs. (15) and (16). Equation (17) is expected to be valid provided that $\Gamma_r + \Gamma_a(n) \ll 1/n^2 - 1/(n+1)^2$. However, see the remarks of Shore concerning this point,¹¹ i.e., it was suggested that this result might have a wider validity.

IV. RESULTS

A. MQDT

In order to facilitate comparison between the two theories, we rewrite Eq. (9) as

where

$$x_{\pm} = \frac{\pi}{\sqrt{2}(\Delta - k_c^2)^{1/2}(1 + W^2)^{1/2}} [(1 + W^2)^{1/2} \pm 1]^{1/2} \quad (19)$$

and

$$W \equiv \Gamma_r / 2(\Delta - k_c^2) \quad (20)$$

as deduced from Eq. (10).

The following cases are thought to be of interest.

(i) *Resonances strongly overlapped due to "large" Γ_r :* $k_c^2 \rightarrow \Delta$, $\Gamma_r > 0$. From Eq. (19), we obtain the following.

(1) If $\Gamma_r \ll 1$, then $x_{\pm} \gg 1$, giving

$$\sigma_{\text{inel}} \simeq \frac{4\pi}{k_c^2} \frac{\alpha\beta x_-}{[\alpha^2 \cos^2 x_+ + \alpha \sin(2x_+) + 2\alpha\beta x_- + (1 + \beta^2) \sin^2 x_+]} \quad (23)$$

This function has peaks when

$$\tan(2x_+) = -2\alpha / (1 + \beta^2 - \alpha^2), \quad (24)$$

i.e., when $x_+ = \pi \operatorname{Re} Z_n$, from Eq. (12). The value of the cross section at the peak is

$$(\sigma_{\text{inel}})_{\text{max}} \simeq \frac{8\pi}{k_c^2} \frac{\alpha\beta x_-}{\{(\alpha^2 + \beta^2 + 1) + 4\alpha\beta x_- - [(1 + \beta^2)^2 + \alpha^4 + 2\alpha^2 - 2\alpha^2\beta^2]^{1/2}\}} \quad (25)$$

Three cases may be distinguished.

(1) $|\alpha| \ll 1$, $|\beta| \ll 1$; from Eqs. (12) and (16), $\Gamma_a(n) \simeq 4\alpha\beta/\pi n^{*3}$ and

$$(\sigma_{\text{inel}})_{\text{max}} \simeq \frac{2\pi x_- / k_c^2}{(x_- + \alpha\beta/2)} \simeq \frac{4\pi\Gamma_r}{k_c^2 \Gamma_a(n)}. \quad (26)$$

(2) $|\alpha| \gg 1$, $|\alpha| \gg |\beta|$; $\Gamma_a(n) = 4\beta/\pi\alpha n^{*3}$ and

$$(\sigma_{\text{inel}})_{\text{max}} \simeq \frac{4\pi/k_c^2 \alpha x_-}{(\beta + 2\alpha x_-)} \simeq \frac{4\pi\Gamma_r}{k_c^2 \Gamma_a(n)}. \quad (27)$$

(3) $|\beta| \gg 1$, $|\beta| \gg |\alpha|$; $\Gamma_a(n) \simeq 4\alpha/\pi\beta n^{*3}$ and

$$(\sigma_{\text{inel}})_{\text{max}} \simeq \frac{4\pi/k_c^2 \beta x_-}{(\alpha + 2\beta x_-)} \simeq \frac{4\pi\Gamma_r}{k_c^2 \Gamma_a(n)}. \quad (28)$$

The value of $(\sigma_{\text{inel}})_{\text{max}}$ is identical in all these three cases. We next consider the IRA predictions, for a similar range of conditions.

B. IRA

(i) *Resonances strongly overlapped due to "large" Γ_r :* $k_c^2 \rightarrow \Delta$, $\Gamma_r > 0$. From Eq. (17), one has that

$$\sigma^{\text{DR}} \simeq \frac{4\pi}{\Delta} \Gamma_r \Gamma_a(1) \sum_{n=1}^{\infty} \frac{1/n^3}{\left[\frac{4}{n^4} + \left[\Gamma_r + \frac{1}{n^3} \Gamma_a(1) \right]^2 \right]}, \quad (29)$$

where we assume that $n = n^*$ and $\Gamma_a(n) \propto n^{-3}$. Upon converting the sum to an integral, this becomes

$$\sigma_{\text{inel}} \simeq \frac{4\pi\alpha\beta}{\Delta} / [1 + (\alpha + \beta)^2]. \quad (21)$$

(2) If $\Gamma_r \gg 1$, then $x_{\pm} \ll 1$ and

$$\sigma_{\text{inel}} \simeq \frac{4\pi^2}{\Delta} \frac{\beta/\alpha}{\sqrt{\Gamma_r}}. \quad (22)$$

(ii) *Isolated-resonance regime:* $\Gamma_r / (\Delta - k_c^2) \ll 1$. This condition implies that both $x_+ \simeq \pi / [(\Delta - k_c^2)]^{1/2}$ and $x_- \simeq (\pi\Gamma_r / \sqrt{2}) / [2(\Delta - k_c^2)]^{3/2}$. Consequently, the inelastic cross section becomes, if $\cos^2 x_+ \gg x_-^2$ and $\sin^2 x_+ \gg x_-^2$ (usually satisfied),

$$\begin{aligned} \sigma^{\text{DR}} &\simeq \frac{2\pi\Gamma_r}{\Gamma_a(1)\Delta} \int_0^1 dy / \left[y^3 + \frac{1}{\Gamma_a(1)^2} (4y^2 + \Gamma_r^2) \right. \\ &\quad \left. + \frac{2y^{3/2}}{\Gamma_a(1)} \right] \\ &\simeq \frac{\pi\Gamma_a(1)}{\Delta} \tan^{-1} \left[\frac{2}{\Gamma_r} \right] + \mathcal{O}(\Gamma_a^2(1)), \end{aligned} \quad (30)$$

for $\Gamma_a(1) \ll 1$.

We have the following two cases.

(1) $\Gamma_r \ll 1$,

$$\sigma_{\text{inel}} \simeq \frac{\pi^2}{2\Delta} \Gamma_a(1). \quad (31)$$

(2) $\Gamma_r \gg 1$; in this case the sum must be done explicitly and gives

$$\sigma_{\text{inel}} = \frac{4.81\pi}{\Delta} \frac{\Gamma_a(1)}{\Gamma_r}. \quad (32)$$

(ii) *Isolated-resonance region:* $\Gamma_r / (\Delta - k_c^2) \ll 1$. From Eq. (17), the maxima of the inelastic cross section are given by

$$(\sigma_{\text{inel}})_{\text{max}} \simeq 4\pi\Gamma_r / k_c^2 \Gamma_a(n). \quad (33)$$

This expression agrees with the MQDT results obtained in Eqs. (26)–(28). We have not established the equivalence of the areas under the resonance peaks, determined by the MQDT and IRA methods. And, indeed, these areas are not, in general, equal. However, having shown that the peak heights are identical, that the widths are identical (by construction), and that the shapes are similar (Lorentzian in the IRA, and nearly Lorentzian in MQDT), we conclude that the areas are almost equal, in general. Explicit

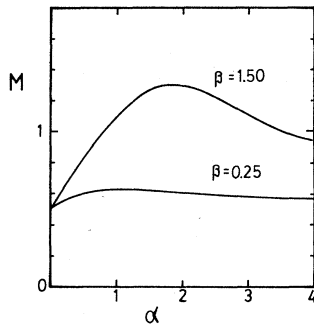


FIG. 1. Plot of the ratio M vs α , for selected values of β ; see Eq. (34).

calculation for a range of α, β values confirms this assertion.

V. DISCUSSION

Comparing the predictions of the MQDT and IRA calculations, we see that in the isolated resonance region of energies the theories are closely similar, independent of the values of α and β ; i.e., see Eqs. (26)–(28) and (33). At energies just below threshold, however, where the resonances are strongly overlapped, the theories can be different. For example, when $k_c^2 \rightarrow \Delta$ and $\Gamma_r \gg 1$ the MQDT predicts $\sigma_{\text{inel}} \propto \Gamma_r^{-1/2}$ whereas the IRA predicts $\sigma_{\text{inel}} \propto \Gamma_r^{-1}$; see Eqs. (22) and (32). More interesting physically is the case of $k_c^2 \rightarrow \Delta$ and $\Gamma_r \ll 1$, for which the ratio of the two cross sections is found to be [from Eqs. (21) and (31)]

$$M \equiv \frac{(\sigma_{\text{inel}})_{\text{IRA}}}{(\sigma_{\text{inel}})_{\text{MQDT}}} = \frac{\pi \Gamma_a(1)}{8\alpha\beta} [1 + (\alpha + \beta)^2], \quad (34)$$

where $\Gamma_a(1)$ is given by Eqs. (12) and (16). For extremes of α and β , such as (1) $|\alpha| \ll 1$ and $|\beta| \ll 1$, (2)

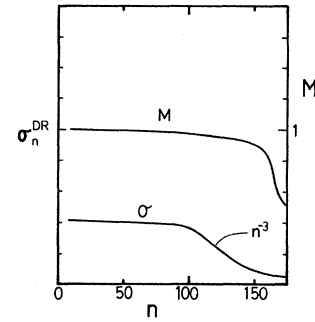


FIG. 2. Estimated dependence of σ_n^{DR} vs n (bottom curve, abscissa in relative units), and M vs n for ions of $Z_I \approx +3$.

$|\alpha| \gg 1$ and $|\alpha| \gg |\beta|$, and (3) $|\beta| \gg 1$ and $|\beta| \gg |\alpha|$, one has that $M \sim 0.5$. If $|\alpha| \approx |\beta| \gg 1$, then $M \sim \ln(2\alpha)$, the worst case. But, if both $|\alpha|$ and $|\beta|$ are of the order of 1 then $M \sim 1$; see Fig. 1. Physically, one expects that $|\alpha| \lesssim 1$ and $|\beta| \lesssim 1$.

Finally, we emphasize that in our experience it is the isolated-resonance region which dominates the DR rate coefficient and DR cross section.¹² For instance, when $Z_I > 15$ then typically $\Gamma_r > \Gamma_a(n)$ for all n . However, for these cases one has that $\Gamma_r \ll Z_I^2/n^3$ so that resonances are very widely spaced. This remains true until n values are attained ($n \equiv n_c \geq 20$) such that for $n > n_c$, σ_n^{DR} becomes negligible. Therefore, for high- Z ions overlapping resonances are unimportant. Now, if instead one considers ions for which $1 \leq Z_I \leq 5$, then $\Gamma_r < \Gamma_a(n)$ until very large n values are reached ($n \equiv n_c \geq 100$). For such cases, usually, $\Gamma_a(n) < Z_I^2/n^3$ too, so that resonances do not overlap until $n > n_c$. However, the contribution to the total DR cross section from all $n \geq n_c$ is again small compared to the contribution from $n < n_c$ since, as before, $\sigma_n^{\text{DR}} \sim n^{-3}$ in the $n \geq n_c$ region. These remarks are illustrated in Fig. 2. Hence, over the entire range of Z_I , it is the isolated-resonance region which dominates σ^{DR} .

¹A. Burgess, *Astrophys. J.* **139**, 776 (1964); **141**, 1588 (1965).

²J. N. Gau and Y. Hahn, *J. Quant. Spectrosc. Radiat. Transfer* **23**, 121 (1980).

³F. Bely Dubau, A. H. Gabriel, and S. Volonte, *Mon. Not. R. Astron. Soc.* **189**, 801 (1979).

⁴U. Fano, *Phys. Rev.* **124**, 1866 (1961).

⁵M. J. Seaton, *Rep. Prog. Phys.* **47**, 167 (1983).

⁶M. J. Seaton and P. J. Storey, in *Atomic Processes and Applications*, edited by P. G. Burke and B. I. Moiseiwitsch (North-Holland, Amsterdam, 1976), Chap. 6.

⁷Y. Hahn, J. N. Gau, R. Luddy, M. Dube, and N. Shkolnik, *J. Quant. Spectrosc. Radiat. Transfer* **24**, 505 (1980).

⁸Y. Hahn, J. N. Gau, R. Luddy, and J. A. Retter, *J. Quant. Spectrosc. Radiat. Transfer* **23**, 65 (1980).

⁹A. P. Hickman, *J. Phys. B* **17**, L101 (1984).

¹⁰Y. Hahn, K. LaGattuta, and D. McLaughlin, *Phys. Rev. A* **26**, 1385 (1982).

¹¹B. W. Shore, *Astrophys. J.* **158**, 1205 (1969).

¹²R. Bell, Ph.D. thesis, University College, London (1979).